Thin Solid Films xxx (2009) xxx–xxx

Contents lists available at ScienceDirect

Thin Solid Films

journal homepage: www.elsevier.com/locate/tsf

Deposition of WN_xC_y thin films for diffusion barrier application using the dimethylhydrazido (2^-) tungsten complex $(CH_3CN)Cl_4W(NNMe_2)$

Hiral M. Ajmera [a], Timothy J. Anderson [a,*], Jürgen Koller [b], Lisa McElwee-White [b,*], David P. Norton [c]

[a] Department of Chemical Engineering, University of Florida, Gainesville, FL 32611, USA
[b] Department of Chemistry, University of Florida, Gainesville, FL 32611, USA
[c] Department of Materials Science and Engineering, University of Florida, Gainesville, FL 32611, USA

ARTICLE INFO

Article history:
Received 18 June 2008
Received in revised form 13 April 2009
Accepted 13 April 2009
Available online xxxx

Keywords:
Chemical vapor deposition
Metallization
Tungsten nitride carbide
Diffusion barrier
X-ray diffraction
Auger electron spectroscopy

ABSTRACT

Tungsten nitride carbide (WN_xC_y) thin films were deposited by chemical vapor deposition using the dimethylhydrazido (2^-) tungsten complex $(CH_3CN)Cl_4W(NNMe_2)$ (**1**) in benzonitrile with H_2 as a co-reactant in the temperature range 300 to 700 °C. Films were characterized using X-ray diffraction (XRD), Auger electron spectroscopy (AES), X-ray photoelectron spectroscopy and four-point probe to determine film crystallinity, composition, atomic bonding, and electrical resistivity, respectively. The lowest temperature at which growth was observed from **1** was 300 °C. For deposition between 300 and 650 °C, AES measurements indicated the presence of W, C, N, and O in the deposited film. The films deposited below 550 °C were amorphous, while those deposited at and above 550 °C were nano-crystalline (average grain size <70 Å). The films exhibited their lowest resistivity of 840 μΩ-cm for deposition at 300 °C. WN_xC_y films were tested for diffusion barrier quality by sputter coating the film with Cu, annealing the $Cu/WN_xC_y/Si$ stack in vacuum, and performing AES depth profile and XRD measurement to detect evidence of copper diffusion. Films deposited at 350 and 400 °C (50 and 60 nm thickness, respectively) were able to prevent bulk Cu transport after vacuum annealing at 500 °C for 30 min.

1. Introduction

The introduction of copper interconnects and low-*k* dielectrics has posed several challenges to their integration into integrated circuits because copper diffuses rapidly in silicon and generates deep energy levels within the band gap, thereby degrading device performance [1]. Barrier films with suitable properties are thus required to prevent incorporation of copper in silicon. The barrier film properties include low resistivity, high thermal and mechanical stability, and good adhesion to adjacent metal and dielectric films [2]. The process for depositing barrier film should be capable of depositing pin-hole free, ultra-thin films with excellent conformality at sufficiently low deposition temperature (<500 °C) to meet the thermal budget constraints of the underlying layers and dielectric film.

Presently, industry employs a physical vapor deposited (PVD) TaN/Ta thin bilayer as a copper diffusion barrier. With the scaling of interconnects, thinner barrier films with excellent conformality in high aspect ratio features will be required. Although ionized-PVD has been able to extend the use of PVD for diffusion barrier deposition by improving the conformality [3], future barrier films will likely be deposited by chemical vapor deposition (CVD) or atomic layer deposition (ALD) [4], which produce films with better conformality than those from PVD. Unfortunately TaN_x films deposited by CVD or ALD [5–9] exhibit high resistivity due to growth of the insulating Ta_3N_5 phase. Furthermore, incorporating a separate diffusion barrier and adhesion layers adds thickness to the barrier scheme as well as an additional processing step.

Binary transition metal compounds, such as WN_x, commonly fail under thermal stress because of film recrystallization [10]. The resulting grain boundaries act as fast diffusion pathways for copper transport leading to failure of the barrier film [2]. The recrystallization temperature can be increased by using ternary refractory metal compounds such as nitride–carbides. The addition of a third element to the binary transition metal compound disrupts the crystal lattice and thus ternary compounds deposited in the amorphous state show a higher onset temperature for recrystallization [11]. To this end, ternary refractory metal compounds such as TiN_xC_y [12], TaN_xC_y [13], and WN_xC_y [14] have been investigated for diffusion barrier application.

In particular, WN_xC_y is a promising material for diffusion barrier application. ALD WN_xC_y films have been demonstrated to be thermally stable after annealing up to 700 °C [15]. The films have good adhesion to Cu and are compatible with dielectric films such as SiO_2 and SiLK™ and etch stop layers such as SiC and Si_3N_4 [16]. The films deposited

* Corresponding authors. Anderson is to be contacted at Department of Chemical Engineering, University of Florida, Gainesville, FL 32611, USA. Tel.: +1 352 392 0947; fax: +1 352 392 9673. McElwee-White, Department of Chemistry, University of Florida, Gainesville, FL 32611, USA. Tel.: +1 352 392 8768; fax: +1 352 846 0296.
E-mail addresses: tim@ufl.edu (T.J. Anderson), lmwhite@chem.ufl.edu (L. McElwee-White).

0040-6090/$ – see front matter © 2009 Elsevier B.V. All rights reserved.
doi:10.1016/j.tsf.2009.04.036

using WF_6, NH_3 and triethylboron also have low resistivity of 300 to 400 μΩ-cm for deposition between 300 and 400 °C. Diffusion barrier testing by the etch pit test showed that 12 nm thick WN_xC_y film prevented copper diffusion after annealing at 550 °C for 30 min [17]. In an electromigration test performed at 325 °C, copper film deposited on WN_xC_y exhibited better electromigration resistance than copper film deposited on PVD Ta [18]. Stress tests performed at 300 °C with a 0.7 MV/cm applied electric field showed that a 5 nm WN_xC_y barrier was able to prevent copper diffusion. These reports support that WN_xC_y is a promising material for diffusion barrier applications.

Most of the reports on ALD WN_xC_y have employed halide chemistry with WF_6 as the tungsten source, NH_3 as the nitrogen source and Et_3B as the carbon source. The WN_xC_y films deposited using halide chemistry showed poor adhesion to SiO_2 (1.5 J/m^2) as measured by the four-point bend test, possibly due to F incorporation at the WN_xC_y/SiO_2 interface [19]. Moreover, there are issues related to the handling and storage of WF_6. An alternative method for deposition of WN_xC_y is thus desirable.

Given the potential of WN_xC_y, we have sought to develop a single source CVD precursor. Challenges of using a single source precursor include producing a film within the composition range of acceptable film conductivity (higher C) and barrier effectiveness (higher N) and at a growth temperature below ~450 °C. We have previously reported deposition of WN_xC_y thin films by CVD from the tungsten imido precursors $Cl_4(RCN)W(NPh)$ (R = CH_3, Ph) (**2a,b**), $Cl_4(RCN)W(NC^iPr)$ (R = CH_3, Ph) (**3a,b**), $Cl_4(RCN)W(NC_3H_5)$ (R = CH_3, Ph) (**4a,b**) and $W(N^iPr)Cl_3[^iPrNC(NMe_2)N^iPr]$ (**5**) [20–23]. We now report the use of the dimethylhydrazido(2−) tungsten complex $(CH_3CN)Cl_4W(NNMe_2)$ (**1**) for deposition of WN_xC_y thin films. Use of the hydrazido ligand was motivated by prior studies in which we observed that the activation energy for film growth depended on the estimated N(imido)–C bond dissociation energies for **2a,b–4a,b** [21]. In the hydrazido derivatives $(CH_3CN)Cl_4W(NNR_2)$ [24], this bond is replaced by an N–N bond, which, to the extent that organic hydrazines are good models, should be relatively weak. In addition, there are literature examples in which hydrazine derivatives were added to the carrier gas during deposition to reduce high valent metal complexes [25–27], a beneficial effect that is also observed for deposition of metal nitride films from hydrazido complexes [28–31]. Although the presence of H_2 as a reductant during our depositions will render reduction by the hydrazido moiety less important than in the literature depositions, which were carried out under Ar [26,27], it could still be beneficial. Utilization of hydrazine derivatives should also result in higher N content in the deposited films. High N content in diffusion barrier films is important as excess N is believed to stuff grain boundaries and improve copper barrier effectiveness.

2. Experimental procedures

2.1. Precursor synthesis

Dimethylhydrazido complex **1** was prepared as described in the literature [24].

2.2. Film growth studies

Film deposition was carried out in a vertical cold-wall CVD reactor, which has been described previously [22]. The solid precursor **1** was dissolved in benzonitrile at a concentration of 7.4 mg/mL. All depositions were carried out at 46.7 kPa pressure for a period of 150 min. The molar flow rate of precursor **1**, H_2 and benzonitrile used in the CVD reactor was constant at 1.16×10^{-6}, 4.09×10^{-2}, and 6.47×10^{-4} mol/min, respectively. The lowest temperature at which film growth could be observed was 300 °C. Films were deposited at substrate temperature between 300 and 700 °C in 50 °C increments.

2.3. Film characterization

Film crystallinity was examined by X-ray diffraction (XRD) using a Phillips APD 3720 system. Cu Kα radiation, generated at 40 kV and 40 mA (1.6 kW), was used for the XRD analysis. The XRD patterns were recorded between 5 and 85° 2θ with step size of 0.05°/step. Film composition was determined by Auger electron spectroscopy (AES) using a Perkin-Elmer PHI 660 Scanning Auger Multiprobe. A 5 kV acceleration voltage and 50 nA beam current was used for the Auger analysis with a beam diameter of 1 μm. The sample surface was cleaned by sputter etching for 30 s using Ar^+ ions. The etch rate for the sputtering was calibrated at 100 Å/min using a tantalum oxide standard. Since no WN_xC_y standard was available, elemental sensitivity factors were used to determine film composition. X-ray photoelectron spectroscopy (XPS) spectra were taken using monochromatic Mg Kα radiation with the X-ray source operating at 300 W (15 kV and 20 mA). The sample surface was sputter etched for 15 min using Ar^+ ions to remove surface contaminants. The etch rate for the XPS system was calibrated at 10 Å/min using a tantalum oxide standard. The pass energy used for XPS multiplex measurement was 35.75 eV and the step size of scans was 0.1 eV per step.

The film thickness was measured by cross-sectional scanning electron microscopy (X-SEM) on a JEOL JSM-6400. The sheet resistance of the deposited films was measured using an Alessi Industries four-point probe. To test diffusion barrier quality, the WN_xC_y films were transferred in air to a multi-target sputter deposition system (Kurt J. Lesker CMS-18) where 100 nm thick Cu films were deposited. The base pressure of the system was 1.3×10^{-4} Pa and deposition was performed at 0.7 Pa with Ar as the sputter deposition gas. The forward sputtering power for the Cu target was 250 W and the film growth rate was 240 Å/min. Annealing of the $Cu/WN_xC_y/Si$ stacks was also performed in the sputter system at a base pressure of 1.3×10^{-4} Pa.

3. Results and discussion

3.1. Film growth by CVD

When CVD growth from **1** was attempted at 400 °C in an inert atmosphere with N_2 carrier gas, the resulting film contained W and O while no C or N was detected by AES. When the reductant H_2 was substituted as the carrier gas for N_2 at the same deposition temperature, the deposited film contained W, N, C and O as determined by AES. Hence, the presence of H_2 facilitates deposition of WN_xC_y thin film from **1**. For growth between 300 and 700 °C, the color of the deposited film varied from golden brown at low deposition temperature to grayish at higher deposition temperature.

The lowest temperature at which film growth was observed from **1** with H_2 as a co-reactant was 300 °C. This minimum growth temperature is lower than that observed for any of the imido precursors **2a,b–4a,b**, with a minimum growth temperature in the range 450 to 475 °C. This result is consistent with the relationship between apparent activation energy for film growth and estimated N(imido)–C bond dissociation energy that we have observed for film growth from **2a,b–4a,b** [21]. If the growth mechanism for **1** is similar to that for **2a,b–4a,b**, then the weaker N–N bond dissociation energy for **1** as compared to **2a,b–4a,b** (based on organic hydrazines as a model for **1** in the same manner as organic amines were used as models for **2a,b–4a,b**) is expected to result in growth at lower temperature.

The growth rate for films deposited from **1** was determined by measuring the film thickness using X-SEM and dividing by deposition time. X-SEM images of the film grown at 400 and 650 °C are shown in Fig. 1. The growth rate increased from 1 Å/min at 300 °C to 13 Å/min for deposition at 450 °C, and then leveled off, decreasing slightly in the growth temperature range 450 to 650 °C. For deposition at 700 °C, the growth rate increased significantly to 38 Å/min suggesting a change in growth mechanism. Fig. 2 depicts the Arrhenius plot for deposition from

Please cite this article as: H.M. Ajmera, et al., Thin Solid Films (2009), doi:10.1016/j.tsf.2009.04.036

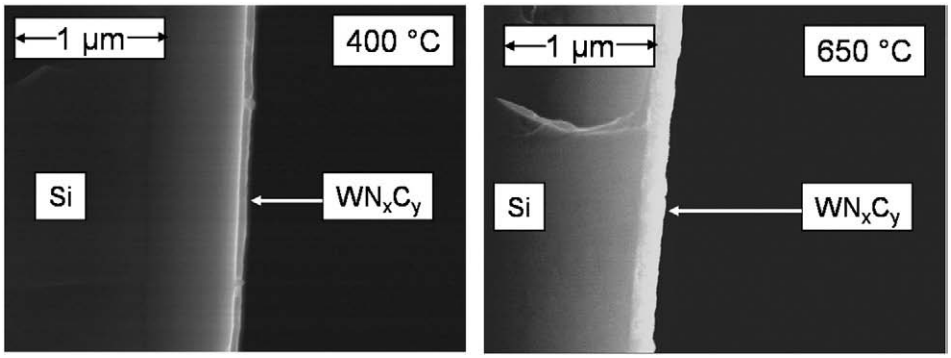

Fig. 1. Scanning electron microscope images for films deposited from **1** at 400 and 650 °C on Si(100) substrate.

1. Film growth rate increased exponentially with temperature between 300 and 450 °C with apparent activation energy of 0.52 eV, suggesting that growth occurs in the surface reaction-limited regime. For film deposited between 450 and 650 °C, the weak temperature dependence is consistent with mass transfer limited growth. A low deposition temperature, <450 °C, is required for Cu barrier application to satisfy thermal budgets and avoid material degradation, while operating in the reaction-limited regime generally produces more conformal films if a uniform surface temperature is established. For a given reaction mechanism and reactor design, the transition temperature from surface to mass transfer limited growth can be increased by changing the operating conditions, most commonly by lowering the operating pressure or increasing the total flow rate. The reaction-limited growth rate observed in this study at 300 °C (1 Å/min) would require a substantial growth time for proposed barrier thicknesses, but the rate can be increased by increasing the inlet precursor concentration. Thus use of precursor **1** for depositing barrier material appears to have suitable growth rate behavior.

3.2. Film composition and atomic bonding

AES results for films deposited using **1** between 300 and 650 °C indicated the presence of W, N, C and O in varying concentration (Fig. 3), whereas films deposited at 700 °C showed the presence of only W, C and O. Bonding of W, N, C and O in the films deposited from **1** between 300 and 700 °C was investigated by XPS (Fig. 4). The deconvolution of the W 4f and 4p XPS peaks for deposition at 300 °C indicates the presence of three different bonding states of W. The first W $4f_{7/2}$ peak at 32.0 eV lies between the reference W peaks of W_2C (ca. 31.6 eV) [32–34] and W_2N (ca. 33.0 eV) [35,36], indicating that the W atom is bonded to both C and N. The second $4f_{7/2}$ peak at 33.4 eV lies between the reference WO_2 peak at ca. 32.9 eV [32,37] and reference W_2O_5 peak at 34.6 eV [37], suggesting that the stoichiometry of tungsten oxide associated with this peak is WO_x ($2<x<2.5$). The third W $4f_{7/2}$ peak at 35.2 eV corresponds well with the reference W $4f_{7/2}$ peak for WO_3 (ca. 35.5 eV) [32,35,37]. The results of the AES and XPS measurements are summarized below.

The films deposited between 300 and 650 °C are W rich, with W content varying between 51 and 63 at.%. In contrast to the W composition variation with growth temperature, the N content in the film shows a maximum value of 24 at.% for deposition at 350 °C. The N content then declines with increasing deposition temperature until it reaches 5 at.% for film grown at 650 °C. The N XPS peak for deposition at 300 °C can be deconvoluted into two peaks. The first N 1s peak at 397.5 eV corresponds well with the reference N 1s peak for N in WN_x film [35,36]. The second peak at 398.8 eV suggests that N is also present in an amorphous state [35]. Between 300 and 600 °C, the N peak can be similarly deconvoluted into a dominant peak around 397.5 eV and a broad shallow peak around 398.5 eV implying that the bulk of N is bonded to W with a small amount of N present in an amorphous phase. This is desirable for diffusion barrier film because excess N at the grain boundaries is believed to improve the diffusion barrier performance. Since N does not form a stable compound with copper, the presence of amorphous N hinders the diffusion of copper along the grain boundaries [38,39]. The film deposited at 700 °C shows no N 1s peak adding to the evidence that the film is WC_x.

The C content of the film remains unchanged at ca. 9 at.% for deposition between 300 and 400 °C. Above 400 °C, the general trend is for the carbon content derived from the precursor and/or benzonitrile solvent [40] to increase with increasing deposition temperature, with a

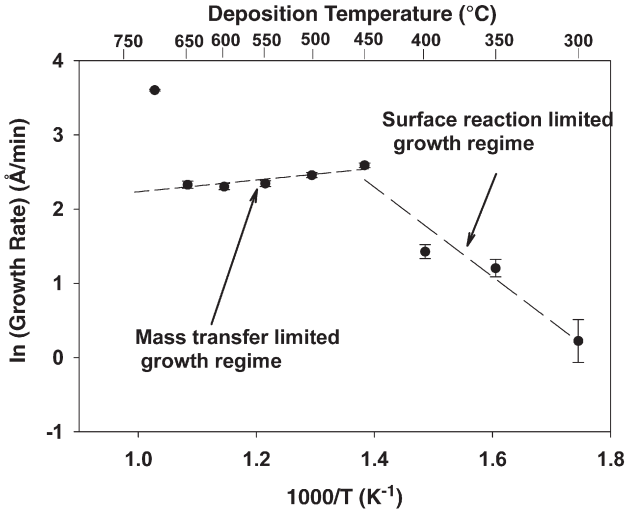

Fig. 2. Arrhenius plot for deposition from **1** on a Si(100) substrate.

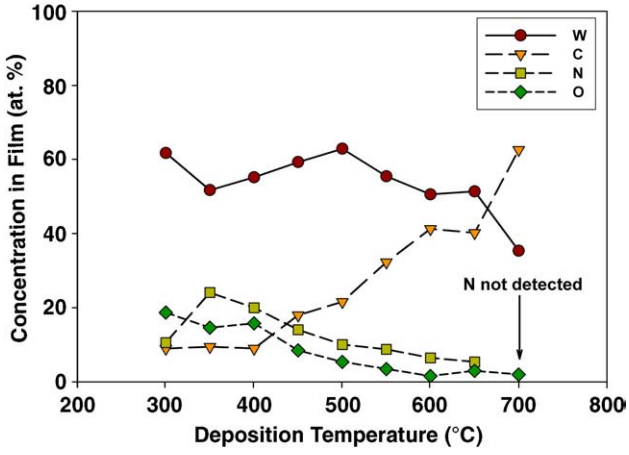

Fig. 3. Composition of films deposited from **1** on Si(100) substrate at different deposition temperature as determined by AES after 0.5 min of sputtering.

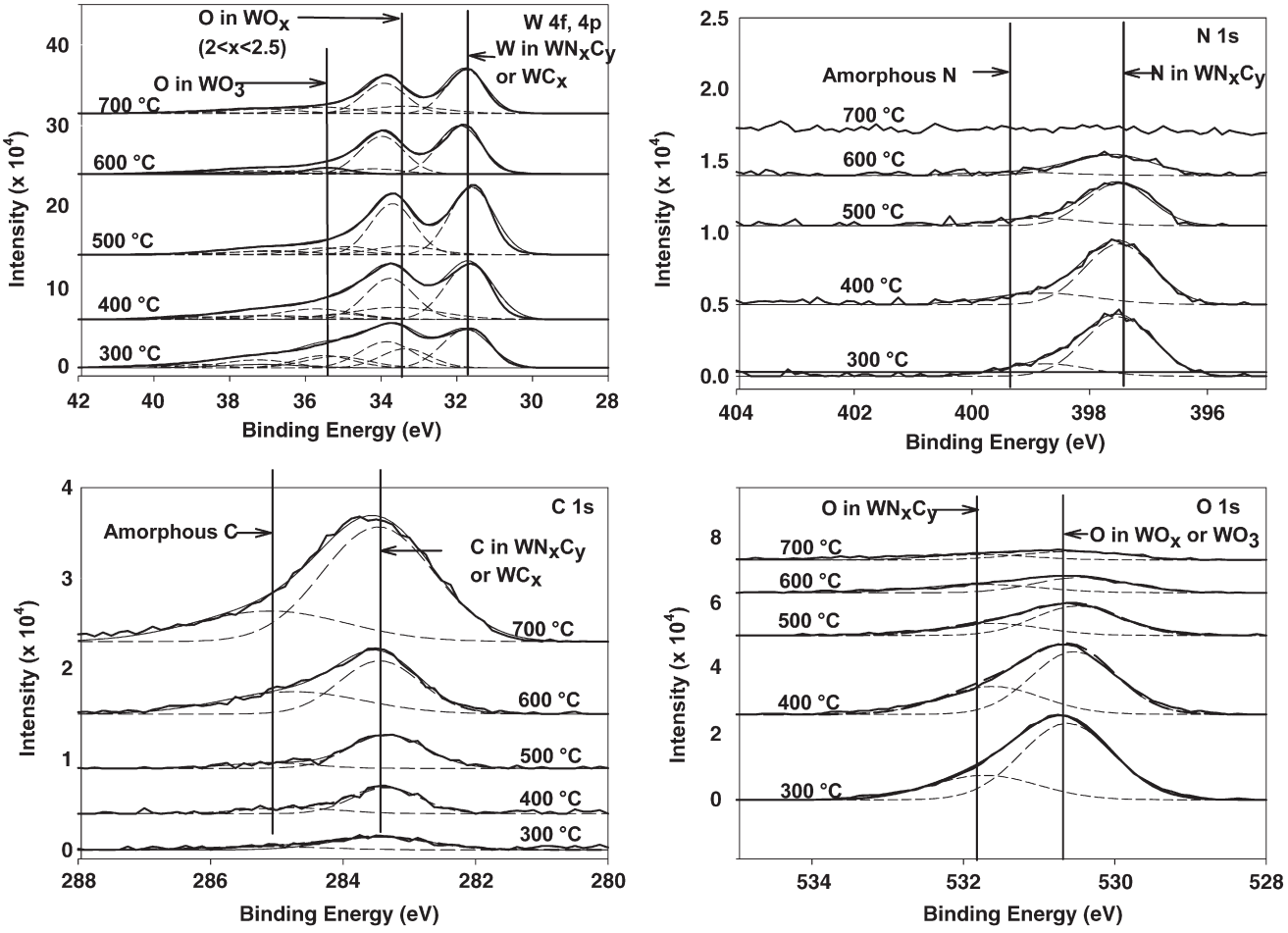

Fig. 4. X-ray photoelectron spectroscopy peak deconvolution for films deposited from **1** between 300 and 700 °C on Si(100) substrate.

significant increase for the film grown at 700 °C. For films deposited between 300 and 700 °C, the C 1s XPS peak can be deconvoluted into two peaks around 283.4 and 285.0 eV. The former peak corresponds to C bonded to W (reference peak at ca. 283.5 eV [32,33]) and the latter peak reflects C in an amorphous state (reference peak at ca. 285.2 eV [32]). Between 300 and 500 °C, the C 1s peak deconvolution shows that the C in the film is predominantly bonded to W with some C present in an amorphous state. For deposition at 600 and 700 °C, however, a much greater proportion of total C in the film is amorphous C. The growth rate data suggests that deposition mechanism changed for the 700 °C run. The AES measurements show that the film grown at this temperature had a considerably lower W content (34 at.%) while the N content is below the detection limit of AES, thus this film contains only WC_x and amorphous carbon.

The O content of the film generally decreases from 19 to 2 at.% as the growth temperature increases to 600 °C and then remains at this low value for growth at 650 and 700 °C. From the XPS measurements, the intensity of the W peak corresponding to WO_x and WO_3 decreases with increasing deposition temperature, which is consistent with the AES results. For deposition at 700 °C, the W peaks can be deconvoluted into WC_x and WO_x peaks without a contribution from WO_3. The O 1s peak for films deposited between 300 and 700 °C can be deconvoluted into two peaks at ca. 530.5 and ca. 531.7 eV. The peak at 530.5 eV corresponds to O in WO_3 (literature value of ca. 530.5 eV [37,41]). The other peak at 531.7 eV represents O bonded to W in sub-stoichiometric WO_x [41]. With an increase in deposition temperature, the peak intensity decreases for O present in both WO_x and WO_3. These results are consistent with chemical equilibrium calculations [42] on the reduction of tungsten oxides in H_2. These calculations suggest that WO_2 is considerably more stable than WO_x ($2.72 \leq x \leq 3$). Of course oxygen incorporation can occur over a range of temperature and gas composition that will yield non-equilibrium reaction extents. Oxygen could be incorporated into the film during growth from several sources including residual gas (O_2 and water vapor) in the reactor and/or impurities in the precursor and carrier gas. It could also be

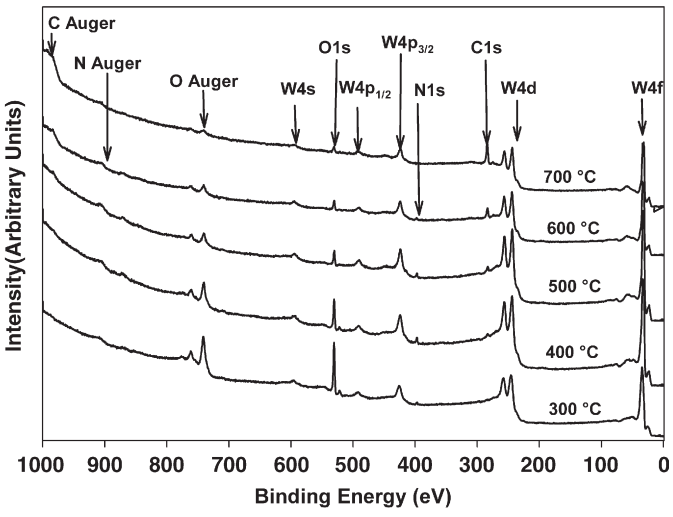

Fig. 5. X-ray photoelectron spectroscopy survey measurements for films deposited from **1** on Si(100) substrate at different deposition temperatures.

Please cite this article as: H.M. Ajmera, et al., Thin Solid Films (2009), doi:10.1016/j.tsf.2009.04.036

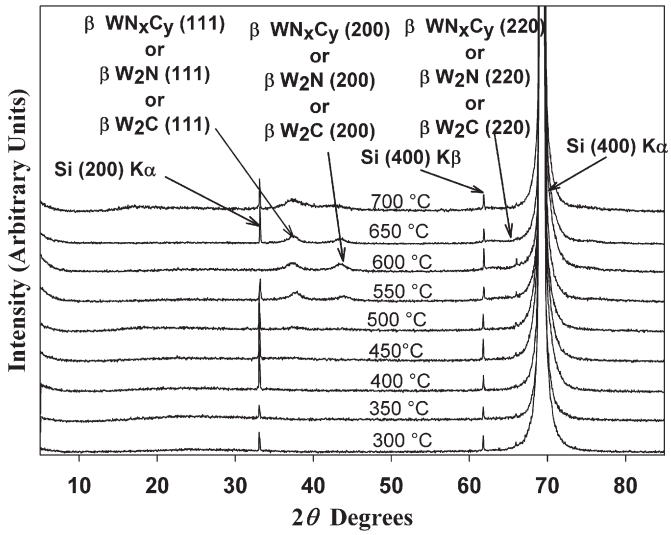

Fig. 6. X-ray diffraction patterns for films deposited from **1** between 300 and 700 °C on Si(100) substrate.

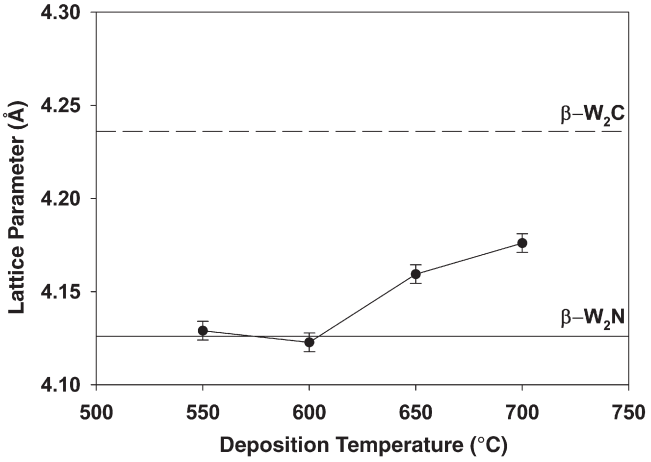

Fig. 7. Lattice parameter for films grown from **1** on Si(100) substrate. Error bars indicate uncertainty in determination of peak position for lattice parameter calculation.

incorporated post growth due to exposure to atmospheric O_2 and water vapor.

Due to the presence of chloride ligands in **1**, the possible presence of chlorine in the films was of interest. XPS was used to analyze for Cl in the film because the W NNN peak in AES spectra overlaps with the Cl LMM peak at ca. 180 eV. Fig. 5 shows the XPS data for films deposited using **1** between 300 and 700 °C. No peaks were observed for either Cl 2s or Cl $2p_{3/2}$ at 270 and 199 eV, respectively, confirming that the chlorine level in the films was lower than the detection limit of XPS (ca. 1 at.%). Of course, small amounts of Cl at the metal/barrier interface can reduce the resistance to electromigration, and this possibility needs to be tested.

The composition of films deposited from **1** provides insight into the effect of the dimethylhydrazido ligand on film N content. Previous work on precursors **2a,b**–**5** has shown that films deposited with H_2 as a co-reactant had low N content (highest value of 12 at.%) [20–23]. One approach to increase the film N content is to use NH_3 as a co-reactant. When **3a,b** was used with NH_3, film N content as high as 23 at.% was observed for deposition at 450 °C [43]. Equivalent N levels, however, can be obtained from hydrazido complex **1** without addition of an external nitrogen source (i.e., 24 at.% of N at 350 °C without the use of co-reactants such as NH_3). This could be due to a low N–N bond dissociation energy for **1**, which would result in a ratio of N–N to W–N cleavage for the hydrazido ligand of **1** that is more favorable than the ratio of C–N to W–N cleavage in the imido complexes **2a,b**–**5**. The outcome would be a corresponding increase in N content for films grown from **1**.

3.3. Film crystallinity

The XRD patterns for films deposited between 300 and 500 °C (Fig. 6) exhibit no peaks attributable to the film, but only peaks associated with the substrate (Si(200) Kα, Si(400) Kα, and Si(400) Kβ reflections at 33.10, 61.75 and 69.20° 2θ, respectively [44]). The absence of other peaks in these patterns suggests that films deposited at 500 °C and below are X-ray amorphous. The XRD patterns for the films deposited between 550 and 650 °C show evidence of crystallinity in the form of two broad peaks that lie between the standard peak positions of β-W_2N (37.74° 2θ for the (111) reflection and 43.85° 2θ for the (200) reflection [45]) and β-W_2C (36.98° 2θ for the (111) reflection and 42.89° 2θ for the (200) reflection [46]), indicating the presence of either the solid solution β-WN_xC_y or a physical mixture of β-W_2N and β-W_2C. XPS results, however, indicate that the film is single phase β-WN_xC_y for deposition between 300 and 650 °C. For deposition at 700 °C, the two peaks at 37.20 and 42.55° 2θ are attributed to the β-W_2C phase since the films contain no detectable N as indicated by AES measurements.

Precursors **1**–**5** have shown very similar behavior for the emergence of crystallinity. The lowest deposition temperature at which polycrystalline films are observed is between 500 and 550 °C for **1**–**5**. One possible explanation is that between 500 and 550 °C, the surface diffusivity of adsorbed species reaches the threshold for formation of crystallites.

3.4. Lattice parameter

Fig. 7 shows the change in lattice parameter with deposition temperature for films deposited from **1**. The (111) peak of β-WN_xC_y exhibited the highest intensity and thus was used for calculating the lattice parameter. Changes in lattice parameter could result from compositional changes or uniform strain. Since the films deposited from **1** are highly disordered with grain size in the nanometer range, compositional change is believed to be the primary factor affecting the lattice parameter. For film deposited at 550 °C, the lattice parameter has a value of 4.13 Å, which is similar to the literature value of the lattice parameter for β-W_2N (4.126 Å). As the deposition temperature is increased from 550 to 600 °C, the lattice parameter value remains almost unchanged at 4.12 Å even though the C content of the film increases by 9 at.%. If the additional C were incorporated on the N sublattice in β-W_2N to form a solid solution, the lattice parameter value would have increased towards the value for W_2C (4.236 Å). An observation to the

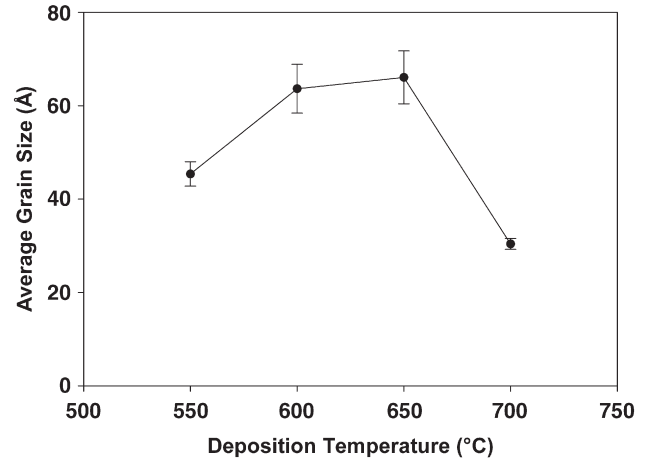

Fig. 8. Average grain size for films grown from **1** at different deposition temperatures on Si(100) substrate.

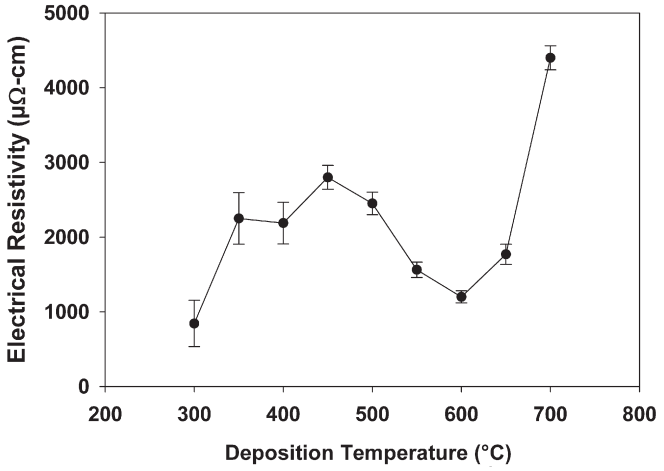

Fig. 9. Change in film resistivity with deposition temperature for films deposited from **1** on Si(100) substrate.

contrary suggests that the additional C is incorporated outside the W sublattice in an amorphous state. For depositions between 600 and 650 °C, the lattice parameter increases from 4.12 to 4.16 Å. In the same temperature range, the overall film composition as determined by AES remains relatively unchanged. The increase in lattice parameter could be due to increase in the concentration of interstitials (C, N and/or O) or a decrease in vacancies on the W sublattice. As deposition temperature is increased to 700 °C, the lattice parameter increases further to 4.18 Å. At 700 °C, the film is β-W_2C as evidenced by AES measurement, but the lattice parameter of 4.18 Å is much lower than the standard lattice parameter of 4.236 Å for β-W_2C, possibly due to a higher W vacancy concentration.

3.5. Average grain size

For polycrystalline diffusion barrier film, grain size is important for barrier effectiveness because grain boundaries provide facile diffusion pathways for copper. If the grain size is on the order of the feature size of the trench or via, the grain boundary could provide a shorter continuous path for diffusion of copper. On the other hand, a nanocrystalline film with grain sizes several orders of magnitude smaller than the feature size would result in a tortuous path for copper diffusion and has a better potential as a diffusion barrier. For the same reason, randomly oriented polycrystals are preferred over a columnar structure.

For the polycrystalline films deposited from **1**, XRD peak broadening was used to determine average crystallite size (Fig. 8) using Scherrer's equation [47]. As a preliminary step, plots of $B\cos\theta$ vs. $\sin\theta$ using the measured peak intensities for (111), (200) and (220) reflections for the films deposited at 550 and 700 °C were horizontal, consistent with attributing line broadening to variations in grain size and not residual strain. Since the (111) reflection was most intense, it

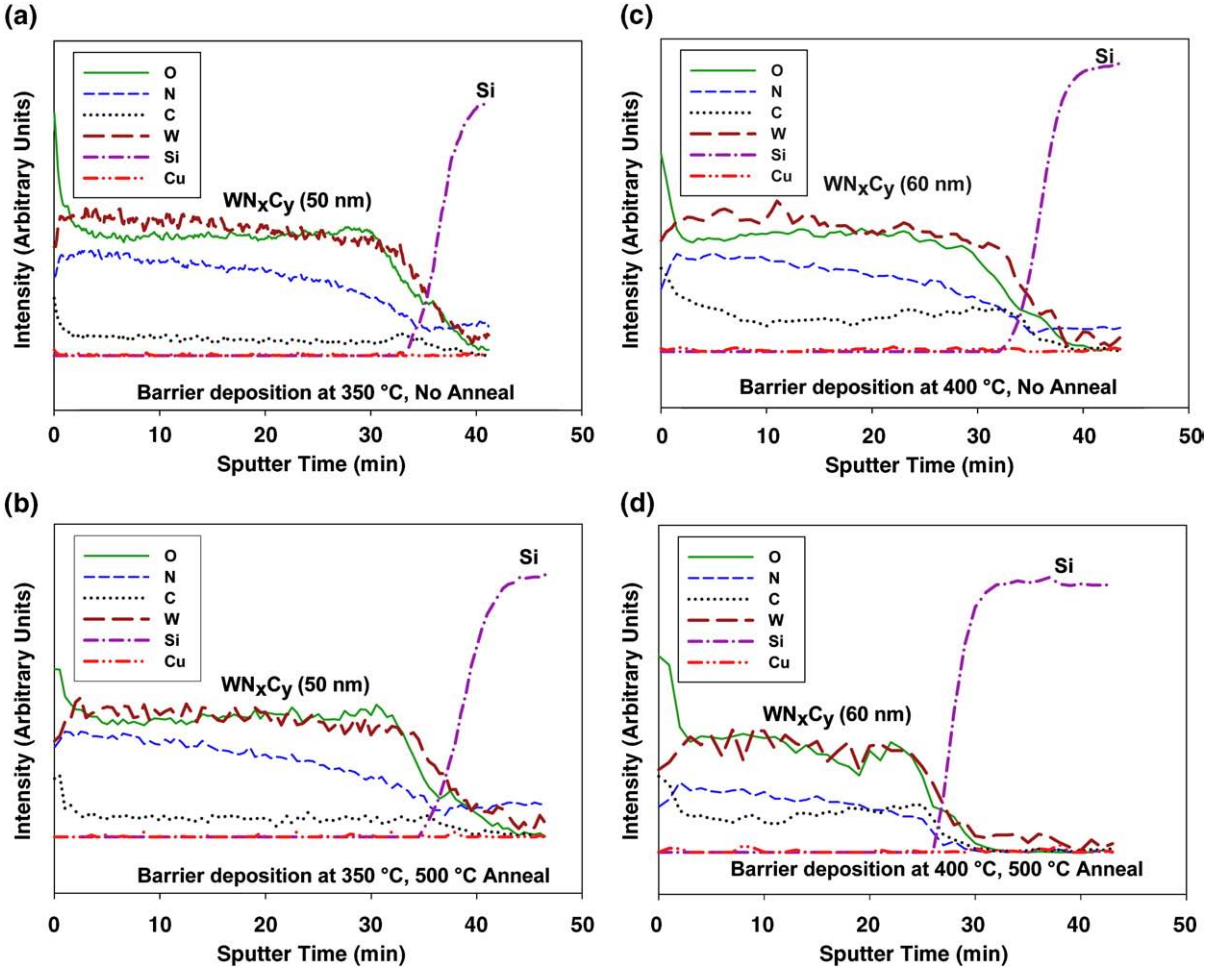

Fig. 10. Pre- and post-anneal AES depth profile of Cu/WN_xC_y/Si (substrate) stack for WN_xC_y film deposited from **1**. After vacuum annealing for 30 min and prior to AES depth profiling, the Cu layer in the Cu/WN_xC_y/Si stack was removed by etching. a) Barrier deposition at 350 °C, no annealing. b) Barrier deposition at 350 °C, annealing at 500 °C. c) Barrier deposition at 400 °C, no annealing. d) Barrier deposition at 400 °C, annealing at 500 °C.

was used to determine the FWHM and estimate average grain size. The estimated average grain size is 45 Å for deposition at 550 °C. Between 550 and 650 °C, the average grain size increases with deposition temperature presumably because the higher surface diffusivity of adsorbed species results in an increase in grain growth. The average grain size, however, decreases to 30 Å for deposition at 700 °C. This decrease in grain size could result from either change in reaction mechanism as evidenced by formation of β-W_2C instead of β-WN_xC_y or higher growth rate for deposition at 700 °C (*vide infra*), which would limit the diffusion and rearrangement of adsorbed species on the substrate surface resulting in deposition of film with smaller grain size. Overall, the average grain size measurement indicates that the films deposited from **1** at and above 550 °C are nano-crystalline with average grain size varying between 30 and 66 Å.

3.6. Film resistivity

Fig. 9 shows the variation of film resistivity with deposition temperature for films deposited from **1**. The film with the lowest resistivity (840 μΩ-cm) was obtained at a deposition temperature of 300 °C. A number of factors lead to lower resistivity of transition metal nitrides and carbides including higher metal ratio, lower vacancy concentration in the metal and non-metal sublattices, metallic bonding states between W and C or N, lower impurity levels (e.g. O), higher film crystallinity and lower porosity [48]. As the deposition temperature is increased from 300 to 350 °C, the film resistivity increases sharply to 2250 μΩ-cm in parallel with the increase in N content of the film. As the growth temperature increases from 450 and 600 °C, the film resistivity gradually decreases from 2800 to 1200 μΩ-cm. The film deposited at 700 °C shows the highest resistivity of 4400 μΩ-cm even though AES results indicate that the film is WC_x, which has low bulk resistivity (22 μΩ-cm at 20 °C) [49]. The high resistivity of this film is consistent with the presence of extensive amorphous C as indicated by the XPS spectrum.

3.7. Diffusion barrier testing

To determine the effectiveness of film deposited from **1** as a Cu diffusion barrier, WN_xC_y films deposited at 350 and 400 °C (50 and 60 nm thick, respectively) were coated with 100 nm PVD Cu. Prior to the deposition of Cu, the barrier film was exposed to atmosphere for approximately 1–2 h. The Cu/barrier/Si stack was annealed in vacuum at 500 °C for 30 min. After annealing, XRD measurement was performed on the Cu/barrier/Si stack to evidence the formation of Cu_3Si formed upon barrier failure. Previous work on films that failed barrier testing showed XRD peaks corresponding to Cu_3Si formation [15,50]. Three-point AES depth profiling was also carried out on an annealed barrier/Si stack obtained after removing the Cu layer by etching with dilute HNO_3. Removal of the Cu layer was necessary to minimize the 'knock-on' effect during sputtering.

Fig. 10 shows the AES depth profile of pre- and post-anneal Cu/WN_xC_y/Si stacks for WN_xC_y films deposited at 350 and 400 °C. For deposition at 350 °C, the post-anneal AES depth profile (Fig. 10b) shows that the Cu signal in barrier film is similar to that observed in the pre-anneal depth profile (Fig. 10a), suggesting that the barrier film was able to prevent bulk Cu diffusion into the Si after annealing. The post-anneal depth profile shows that there is sharp barrier/Si interface, which is similar to that observed in the pre-anneal profile. The XRD patterns of the pre- and post-annealed film stacks shown in Fig. 11 indicate peaks corresponding to Cu and Si with no indication of Cu_3Si. Thus, both AES and XRD measurements indicate that a 50 nm barrier film deposited at 350 °C was able to prevent bulk Cu diffusion after annealing at 500 °C in vacuum for 30 min. Furthermore, the XRD pattern shows that PVD copper deposition on WN_xC_y has a preferred orientation of (111). This is highly desirable because transport along the (111) direction in Cu is more

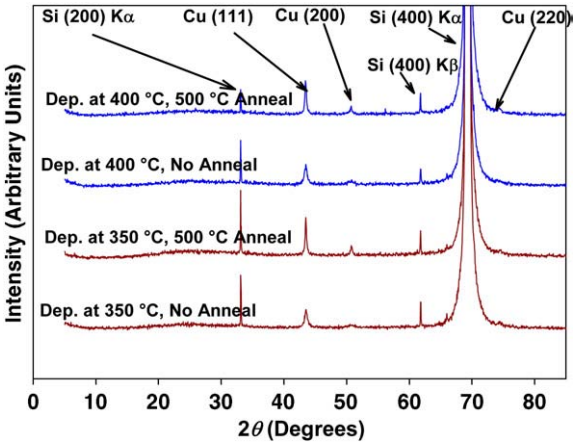

Fig. 11. Pre- and post-anneal XRD measurement of Cu (100 nm)/WN_xC_y/Si (substrate) stack for WN_xC_y film deposited from **1** at 350 and 400 °C.

electromigration resistant as compared to other directions [51]. Similar results were obtained for films deposited at 400 °C (Fig. 10 c and d).

4. Conclusions

It has been demonstrated that the tungsten hydrazido complex $(CH_3CN)Cl_4W(NNMe_2)$ (**1**) can be used with H_2 to deposit WN_xC_y thin films in an aerosol assisted CVD system. The H_2 co-reactant is required for deposition of WN_xC_y as experiments with **1** in inert atmosphere (N_2 carrier gas) resulted in deposition of tungsten oxide films. The lowest temperature at which film growth was observed from **1** was 300 °C. Overall, amorphous film deposition was observed for growth below 550 °C. Films deposited with **1** between 300 and 650 °C consisted of W, N, C and O as determined by AES and no Cl impurity was detected by XPS. The highest N content for films deposited from **1** (24 at.%) was significantly higher than that obtained for films deposited from the analogous tungsten imido complexes **2a,b**–**5** (highest value of 14 at.%), suggesting that the hydrazido ligand contributes to nitrogen incorporation. Importantly, a small amount of amorphous N was detected by XPS. Films showed high resistivity, varying between 840 and 4400 μΩ-cm. XPS results indicate that films deposited at 300 and 400 °C were WN_xC_y with a significant amount of WO_x and WO_3 along with small amounts of amorphous N and C. For deposition at 500 and 600 °C, the bulk of the film was WN_xC_y with a small amount of WO_x/WO_3 and an increased amount of amorphous C. The film deposited at 700 °C consists of WC_x along with a small amount of WO_x and a significantly higher amount of amorphous C. Diffusion barrier testing shows that 50 nm WN_xC_y films deposited at 350 °C and 60 nm WN_xC_y deposited at 400 °C were able to prevent bulk Cu diffusion after annealing at 500 °C in vacuum for 30 min.

Acknowledgements

We thank the National Science Foundation for support under NSF-CRC grant CHE-0304810. Special thanks to the Major Analytical Instrumentation Center (MAIC) at the University of Florida for assistance with XRD, AES and X-SEM analysis.

References

[1] A. Broniatowski, Phys. Rev. Lett. 62 (1989) 3074.
[2] A.E. Kaloyeros, E. Eisenbraun, Ann. Rev. Mat. Sci. 30 (2000) 363.
[3] S.M. Rossnagel, J. Hopwood, Appl. Phys. Lett 63 (1993) 3285.
[4] ITRS, International SEMATECH, Austin, TX, 2006.
[5] S.L. Cho, K.B. Kim, S.H. Min, H.K. Shin, Mater. Res. Soc. Conf. Proc. 514 (1998) 531.
[6] K.I. Choi, B.H. Kim, S.W. Lee, J.M. Lee, W.S. Song, G.H. Choi, U.I. Chung, J.T. Moon, IEEE Interconnect Technology Conf. Proc. (2003) 129.

Please cite this article as: H.M. Ajmera, et al., Thin Solid Films (2009), doi:10.1016/j.tsf.2009.04.036

[7] E. Eisenbraun, O. van der Straten, Z. Yu, K. Dovidenko, A. Kaloyeros, IEEE Interconnect Technology Conf. Proc, 2001, p. 207.
[8] R. Fix, R.G. Gordon, D.M. Hoffman, Chem. Mat. 5 (1993) 614.
[9] M.H. Tsai, S.C. Sun, H.T. Chiu, C.E. Tsai, S.H. Chuang, Appl. Phys. Lett. 67 (1995) 1128.
[10] M. Uekubo, T. Oku, K. Nii, M. Murakami, K. Takahiro, S. Yamaguchi, T. Nakano, T. Ohta, Thin Solid Films 286 (1996) 170.
[11] M.A. Nicolet, I. Suni, M. Finetti, Solid State Technol. 26 (1983) 129.
[12] S. Bocharov, Z.P. Zhang, T.P. Beebe, A.V. Teplyakov, Thin Solid Films 471 (2005) 159.
[13] E.R. Engbrecht, Y.M. Sun, S. Smith, K. Pfiefer, J. Bennett, J.M. White, J.G. Ekerdt, Thin Solid Films 418 (2002) 145.
[14] K.S. Kim, M.S. Lee, S.S. Yim, H.M. Kim, K.B. Kim, H.S. Park, W. Koh, W.M. Li, M. Stokhof, H. Sprey, Appl. Phys. Lett 89 (2006) 081913.
[15] J.Y. Kim, S. Seo, D.Y. Kim, H. Jeon, Y. Kim, J. Vac. Sci. Tech. A 22 (2004) 8.
[16] W.M. Li, K. Elers, J. Kostamo, S. Kaipio, H. Huotari, M. Soininen, P.J. Soininen, M. Tuominen, S. Haukka, S. Smith, W. Besling, IEEE Inter. Interconnect Tech. Conf., 5th (2002) 191.
[17] S.H. Kim, S.S. Oh, H.M. Kim, D.H. Kang, K.B. Kim, W.M. Li, S. Haukka, M. Tuominen, J. Electrochem. Soc. 151 (2004) C272.
[18] S. Smith, G. Book, W.M. Li, Y.M. Sun, P. Gillespie, M. Tuominen, K. Pfeifer, IEEE Interconnect Technology Conf. Proc. (2003) 135.
[19] S. Smith, W.M. Li, K.E. Elers, K. Pfeifer, Microelec. Eng. 64 (2002) 247.
[20] H.M. Ajmera, A.T. Heitsch, O.J. Bchir, T.J. Anderson, L.L. Reitfort, L. McElwee-White, J. Electrochem. Soc. 155 (2008) H829.
[21] O.J. Bchir, K.M. Green, H.M. Ajmera, E.A. Zapp, T.J. Anderson, B.C. Brooks, L.L. Reitfort, D.H. Powell, K.A. Abboud, L. McElwee-White, J. Am. Chem. Soc. 127 (2005) 7825.
[22] O.J. Bchir, K.M. Green, M.S. Hlad, T.J. Anderson, B.C. Brooks, C.B. Wilder, D.H. Powell, L. McElwee-White, J. Organomet. Chem. 684 (2003) 338.
[23] O.J. Bchir, S.W. Johnston, A.C. Cuadra, T.J. Anderson, C.G. Ortiz, B.C. Brooks, D.H. Powell, L. McElwee-White, J. Cryst. Growth 249 (2003) 262.
[24] J. Koller, H.M. Ajmera, K.A. Abboud, T.J. Anderson, L. McElwee-White, Inorg. Chem. 47 (2008) 4457.
[25] D. A. Wierda, C. Amato-Wierda, Proc. Electrochem. Soc. 2000-13 (2000) 497.
[26] C. Amato-Wierda, D.A. Wierda, J. Mater. Res. 15 (2000) 2414.
[27] C. Amato-Wierda, E.T. Norton Jr., D.A. Wierda, Mat. Res. Soc., Symp. Proc. 606 (2000) 91.
[28] J.T. Scheper, P.J. McKarns, T.S. Lewkebandara, C.H. Winter, Mater. Sci. Semicond. Process 2 (1999) 149.
[29] A. Baunemann, Y. Kim, M. Winter, R.A. Fischer, J. Chem Soc., Dalton Trans. (2006) 121.
[30] D. Gaess, K. Harms, M. Pokoj, W. Stolz, J. Sundermeyer, Inorg. Chem. 46 (2007) 6688.
[31] E. Sebe, M.J. Heeg, C.H. Winter, Polyhedron 25 (2006) 2109.
[32] J. Luthin, C. Linsmeier, J. Nucl. Mater. 290–293 (2001) 121.
[33] Y.M. Sun, S.Y. Lee, A.M. Lemonds, E.R. Engbrecht, S. Veldman, J. Lozano, J.M. White, J.G. Ekerdt, I. Emesh, K. Pfeifer, Thin Solid Films 397 (2001) 109.
[34] M.B. Zellner, J.G.G. Chen, Catal. Today 99 (2005) 299.
[35] T. Nakajima, K. Watanabe, N. Watanabe, J. Electrochem. Soc. 134 (1987) 3175.
[36] Y.G. Shen, Y.W. Mai, Mater. Sci. Eng A288 (2000) 47.
[37] A. Katrib, F. Hemming, P. Wehrer, L. Hilaire, G. Maire, J. Elect. Spect. Rel. Phenom. 76 (1995) 195.
[38] B.M. Ekstrom, S. Lee, N. Magtoto, J.A. Kelber, Appl. Surf. Sci. 171 (2001) 275.
[39] N. Shamir, J.C. Lin, R. Gomer, Surf. Sci. 214 (1989) 74.
[40] O.J. Bchir, K.M. Green, M.S. Hlad, T.J. Anderson, B.C. Brooks, L. McElwee-White, J. Cryst. Growth 261 (2004) 280.
[41] G. Leftheriotis, S. Papaefthimiou, P. Yianoulis, A. Siokou, D. Kefalas, Appl. Surf. Sci. 218 (2003) 276.
[42] L. Sha, Z.J. Qiu, Int. J. Refract. Met. Hard Mater. 26 (2008) 362.
[43] O.J. Bchir, K.C. Kim, T.J. Anderson, V. Craciun, B.C. Brooks, L. McElwee-White, J. Electrochem. Soc. 151 (2004) G697.
[44] Silicon Diffraction Pattern; Card # 27-1402, Joint Committee on Powder Diffraction Standards, 1996.
[45] Beta Tungsten Nitride Diffraction Pattern; Card # 25-1257, Joint Committee on Powder Diffraction Standards, 1996.
[46] Beta Tungsten Carbide Diffraction Pattern; Card # 25-1316, Joint Committee on Powder Diffraction Standards, 1996.
[47] B.D. Cullity, S.R. Stock, Elements of X-ray Diffraction, 3rd ed., Prentice Hall, Upper Saddle River, NJ, 2001, p. 664.
[48] L.E. Toth, in: J.L. Margrave (Ed.), Transition Metal Carbides and Nitrides, vol. 7, Academic Press, New York, 1971, p. 279.
[49] H.O. Pierson, Handbook of refractory carbides and nitrides: properties, Characteristics, Processing and Applications, Noyes Publications, Westwood, NJ, 1996, p. 340.
[50] D.J. Kim, Y.B. Jung, M.B. Lee, Y.H. Lee, J.H. Lee, J.H. Lee, Thin Solid Films 372 (2000) 276.
[51] H. Lee, S.D. Lopatin, Thin Solid Films 492 (2005) 279.

Please cite this article as: H.M. Ajmera, et al., Thin Solid Films (2009), doi:10.1016/j.tsf.2009.04.036